ELSEVIER

Journal of Crystal Growth 230 (2001) 40–47

JOURNAL OF CRYSTAL GROWTH

www.elsevier.com/locate/jcrysgro

Convective interaction and instabilities in GaAs Czochralski model

V.I. Polezhaev*, O.A. Bessonov, N.V. Nikitin, S.A. Nikitin

Laboratory of the Mathematical and Physical Modeling in Fluid Dynamics, Institute for Problems in Mechanics, Russian Academy of Sciences (RAS), Prospect Vernadskogo 101, b1, 117526 Moscow, Russia

Abstract

Instability and temperature oscillations in the melt for idealized Czochralski model for typical parameters of the semiisolating GaAs crystal growth configuration are studied. Critical Gr and Re numbers are determined using linear stability analysis and direct numerical simulation. The impact of the height of the melt on convection structure and critical Gr number are studied. Microgravity alternatives for damping of the temperature oscillations are discussed.

Keywords: A1. Computer simulation; A1. Convection; A1. Heat transfer; A1. Instabilities; A2. Czochralski method; B1. Gallium compounds

1. Introduction

Fluid flow in the melt for the so-called idealized or hydrodynamical model of Czochralski growth has been studied for more than 25 years (see, for instance, Refs. [1–5] and references cited therein). The corresponding system of the governing parameters is a multiparametrical one even for unicomponent melt flow containing geometrical and dynamical parameters for forced and gravity-driven convection, physical properties, and boundary conditions, which are important for convection. A problem of fluid flow in this model initiates the analysis of nonlinear interaction, temperature oscillations for gravity-driven and rotational low Prandtl melt flow as a basic fluid dynamics problem.

The study, in this paper, is focused on critical parameters for onset of oscillations induced by forced and natural gravity-driven convection in axisymmetric and three-dimensional (3D) cases for a concrete range of technological configuration related to the LEC semiisolating GaAs crystal growth and comparison of the possibilies to eliminate or control temperature oscillations in the melt.

2. Statement of the parametrical analysis and overview

The problem formulation and a range of problem parameters are described in Refs. [4–8]. The geometry of the problem involves a vertical cylindrical crucible with radius R_c filled with a melt upto a height H (Fig. 1). The crucible can rotate with a constant angular velocity Ω_c and it is in a constant gravitational field with acceleration g. A crystal of radius R_s is mounted in the center of

*Corresponding author. Tel.: +7-095-434-3283; fax: +7-095-938-2048.

E-mail addresses: polezh@ipmnet.ru (V.I. Polezhaev).

0022-0248/01/$ - see front matter
PII: S0022-0248(01)01317-3

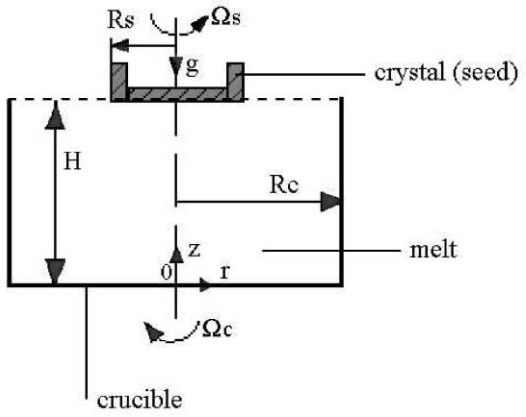

Fig. 1. Scheme of the idealized Czochralski growth.

the upper free surface. The crystal can be rotated with a constant angular velocity Ω_s. It is supposed that the temperature of the crystal surface T_s is constant. The temperature of crucible side wall and crucible bottom is T_c. The melt surface between the crystal and crucible wall is assumed to be shear-free, plane and adiabatic. It is supposed that the melt is Boussinesq fluid. Unsteady Navier–Stokes equations in velocities–pressure formulation and temperature equation are solved in a cylindrical coordinate system, both for axisymmetric and 3D cases [4–8]. The set of non-dimensional governing parameters of the problem consists of two geometrical parameters, H/R_c and R_s/R_c, two Reynolds numbers $\mathrm{Re}_s = \Omega_s R_c^2/\nu$ and $\mathrm{Re}_c = \Omega_c R_c^2/\nu$, Grashof number $\mathrm{Gr} = g\beta(T_c - T_s)R_c^3/\nu^2$, Prandtl number $\mathrm{Pr} = \nu/\kappa$, and parameters γ, γ_0 characterizing the type of boundary and initial conditions. Therefore, a typical characteristic (for instance, an amplitude of the temperature oscillations, a value of macro-inhomogeneity, etc.) of the fluid flow/transport in the melt for Czochralski model may be written as follows:

$$A = f(\mathrm{Re}_c, \mathrm{Re}_s, H/R_c, R_s/R_c, \mathrm{Gr}, \mathrm{Pr}, \gamma, \gamma_0). \quad (1)$$

The problem parameters are extremely different for most of the published works because a number of peculiarities exists for crystal growth technologies. For instance, typical-semiconductor ($\mathrm{Pr} \ll 1$) configurations use counterrotation for crystal and crucible. However, for GaAs configuration, bottom heating [8–13], and for silicon, bottom cooling [14] are used. In case of oxides ($\mathrm{Pr} \gg 1$), adiabatic bottom and rotation of crystal are used [3]. There are different configurations in cases where special liquids are used for modeling, for instance, water ($\mathrm{Pr} = 7$) [15,16], alcohol ($\mathrm{Pr} = 15$) [16], silicon oil ($\mathrm{Pr} = 890$) [17], NaCl–$CaCl_2$ melt ($\mathrm{Pr} = 0.5$) [18]. Wheeler [19] proposed as a benchmark an axisymmetric model with parameters $H/R_c = 1.0$, $R_s/R_c = 0.4$, $\mathrm{Pr} = 0.05$, linear temperature distribution along the melt surface and different Re_s, Re_c and Gr. (see the results of calculations in Refs. [20,4,5]). However, this configuration does not cover the typical range of parameters for the GaAs configuration.

3. Idealized LEC GaAs crystal growth configuration

Typical configuration for the LEC was proposed for systematic research in this paper (see, for instance, Refs. [8–13,21,22]). The temperature on the bottom is the same as on the side wall, $T_c = T_b$, and the melt surface is supposed to be shear-free and adiabatic. It should be noted that thermocapillary phenomena are not taken into account in this paper because they do not seem to be an important factor for GaAs LEC technology, as was discussed in Ref. [10]. The geometrical parameters are characterized by the values $H = 4.0$ cm, $R_s = 4.0$ cm, $R_c = 7.0$ cm. A dynamical regime is typical for GaAs growth counterrotation with faster rotation of the crucible: $\Omega_s = 6$ rpm, $\Omega_c = -16$ rpm. A typical temperature difference between the crystal and crucible is 30°. The corresponding non-dimensional parameters are as follows: $H/R_c = R_s/R_c = 0.578$, $\mathrm{Pr} = 0.07$, $\mathrm{Gr} = 7.8 \times 10^7$, $\mathrm{Re}_s = 6 \times 10^3$, $\mathrm{Re}_c = -1.6 \times 10^4$.

4. Numerical methods and codes

New tools for modeling on the basis of unsteady Navier–Stokes equations developed during the last years represent the following hierarchy.

(1) Common type PC-based system "COMGA" and computer laboratory on the basis of

Navier–Stokes equations which includes most of the elementary technologically important heat and mass transfer processes. Finite difference schemes in the vorticity/stream-function formulation are used in this version of the system. The system and computer laboratory is efficient for the initial stage of research and education and is used now for student training. More detailed description is given in Ref. [6].

(2) Two types of specialized axisymmetric Czochralski models are developed. The first is based on a system "COMGA" and is named "INTEX". It includes a variation of geometry, crystal, crucible rotation, gravity-driven and Marangoni convection for fluids with different Prandtl numbers. More details and benchmark examples can be found in Refs. [7,8]. This system was used for parametric analysis presented below in Sections 5–7. The second type of the axisymmetric codes has the same formulation and possibilities as the first one, but is not supplied by so friendly an interface as the "COMGA" is. This system is used mainly in special cases, for instance, to calculate a basic flow for subsequent linear stability analysis.

(3) For direct numerical simulations of 3D equations for Czochralski model, two numerical codes are developed. The first one is a spectral/difference method, which is described in detail in the paper [4]. The second one is based on a finite-volume scheme for velocity–pressure formulation.

(4) The code for 3D linear stability analysis of fluid flow in an idealized Czochralski model [4] including procedures for the calculation of axisymmetric flow and temperature fields, input of the 3D disturbances and calculation of the 3D disturbances evolution.

5. Crystal and crucible rotation without thermal convection

The computer system "INTEX" with 81×81 grids on non-uniform mesh is used for this case. Steady state temperature and flow fields due to forced convection only ($\mathrm{Gr} = 0$, $\Omega_s = 6$ rpm, $\Omega_c = -16$ rpm) correspond to zero gravity. A classical Taylor–Praudman-type of flow may be recognized on the picture of stream function. Typical diffusion-type isotherms structure may be recognized in $r - z$ plane. However, 3D stability analysis shows that forced flow is definitely unstable. It was shown, using the linear stability analysis technique, that critical speed rotation of the crystal in 3D case $(\Omega_s)_c = 7.7$ rpm. It corresponds to the critical $\mathrm{Re}_s = 7.7 \times 10^3$, which is more than an order less than for an infinite disc. The reason for this fact is an enclosure of a crucible. This critical Ω_s value is higher than the industrial value 6.0 rpm. It confirms that the crystal rotation is not the reason for instability in the 3D case. However, the critical value of the crucible rotation $(\Omega_c)_c$ is found to be about 1.2 rpm ($\mathrm{Re}_c = 1.2 \times 10^3$). This value is more than 10 times lower than the industrial one (16 rpm). Direct numerical simulation on the basis of the 3D model for $\mathrm{Gr} = 0$, $\Omega_s = 6$ rpm, $\Omega_c = -16$ rpm shows an oscillatory azimuthal flow. Therefore, flow instability in this case must exist even for zero gravity.

6. Thermal gravity-driven convection

Fig. 2 shows the temporal evolution of the thermal convection for the basic case obtained by direct numerical simulation of ground-based convection without rotation ($\mathrm{Gr} = 7.8 \times 10^7$, $\Omega_s = \Omega_c = 0$) with the use of the "INTEX" computer system. A strongly non-uniform mesh with 81×81 grids was used in this case.

One can recognize two kinds of thermal convection mechanisms in the crucible: (a) local thermals due to the instantaneous crystal cooling from above and (b) global circulation due to the side heating. However, local mechanism in the form of thermals dominates in this case only at the initial stage (till about 10–15 s). Unsteady thermals structure may be one of the possible and important mechanisms of thermal convection. It was observed in water on the suddenly heated bottom [23]. Realization of thermals by computer system "COMGA" was done in Ref. [6]. A similar structure of thermals, penetrated from above the cooling water surface was reported in Ref. [24]. As reported in Ref. [25], unsteady thermals structure is one of the possible and important mechanisms

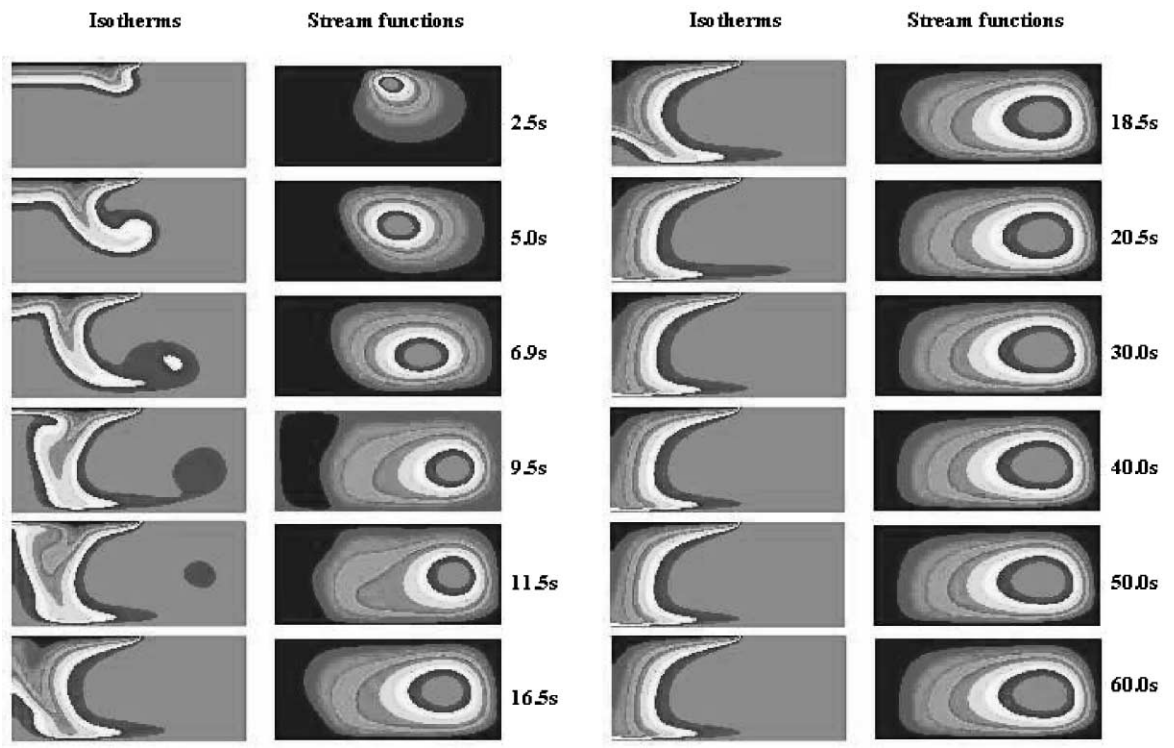

Fig. 2. Evolution of the thermal convection in axisymmetric case ($Gr = 7.8 \times 10^7$, $\Omega_s = \Omega_c = 0$). Values on the right show dimensional time in seconds.

of thermal convection in oxide melt which is characterized by the high Pr number, but not in the semiconductor melt. This conclusion corresponds to the long-term behavior of thermal convection shown in Fig. 2, where global type of convection from the heating side dominates. It should be noted that this situation is typical only for the low Pr number melt. High Pr number experiments show regular oscillations induced by thermals near above the cooling front, and it corresponds to calculations reported in Ref. [25]. Long-term regime in Fig. 2 is a steady state one for axisymmetric case in accordance with the estimation of the critical Gr number for this case. Using parametrical calculations on the basis of axisymmetric model with variation of the Grashof number, critical Gr number for onset of the oscillations was calculated as $Gr = 1.5 \times 10^8$. Therefore, convective regime without rotation in the axisymmetric case should be steady for the basic level $H = 4\,\text{cm}$.

However, thermal convection strongly depends on the melt level. Fig. 3 shows the calculation of convection for different heights of the melt level. The dashed line here shows critical Grashof numbers for the axisymmetric case which is more stable. For instance, the critical Grashof number for 3D convection in the configuration discussed here for $H = 4\,\text{cm}$ was found to be 2.5×10^6 which is significantly smaller than $Gr_c = 1.5 \times 10^8$ for the axisymmetric case. Therefore, in the 3D case, the oscillatory regime must be realized instead of the steady state one in the axisymmetric case.

For the control of temperature oscillations in the melt, the change of the leading convective mechanism depending on the height is very important. Due to the bottom heating Rayleigh–Bernard mechanism of instability in the form of convective cells dominates for small H (area a in Fig. 3). This mechanism has a local nature and produces a transport in a direction from front to

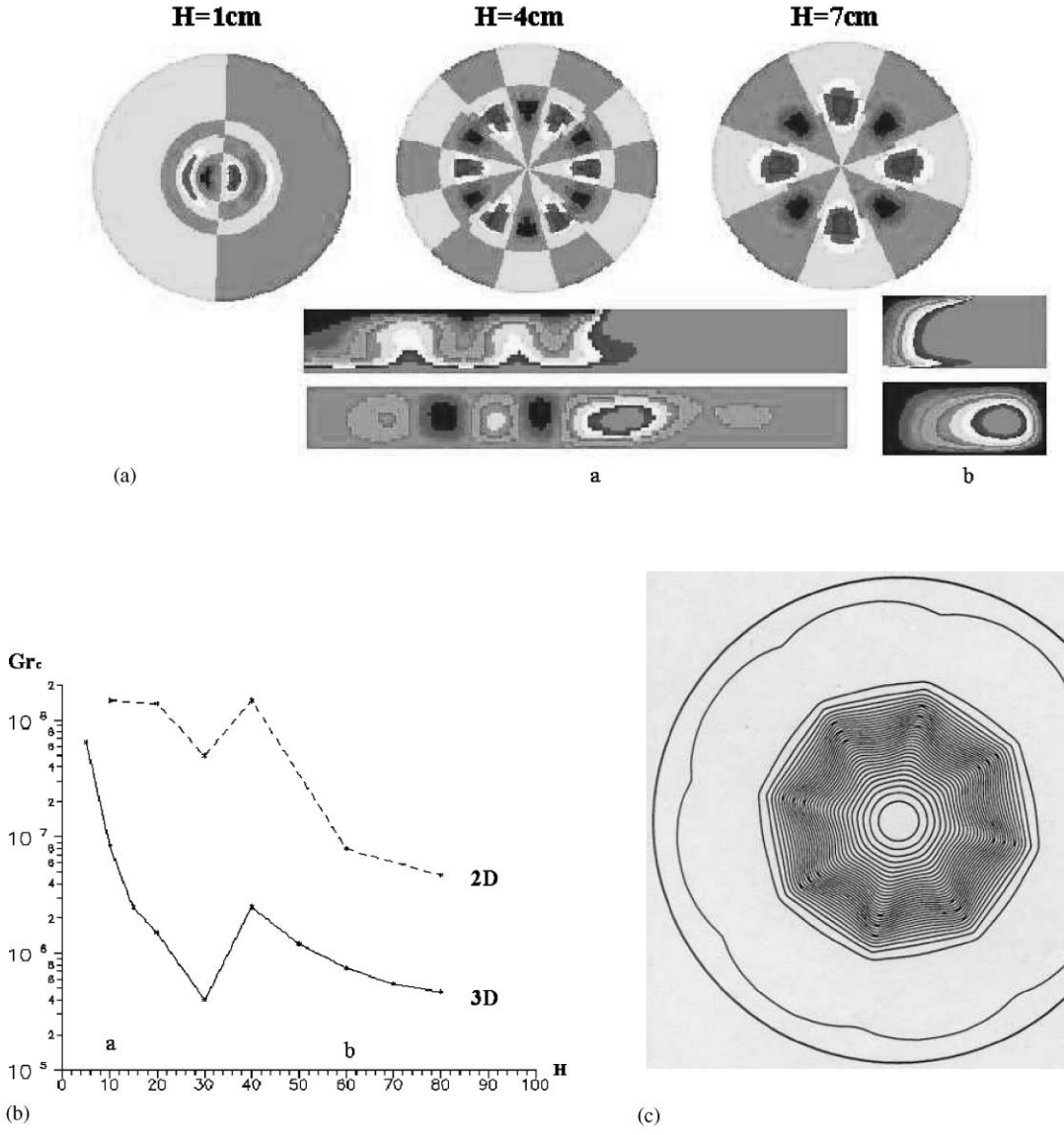

Fig. 3. (a, b) Critical Grashof numbers for the onset of oscillations, temperature and flow patterns for thermal convection ($\Omega_s = \Omega_c = 0$) in axisymmetric and 3D cases for different heights of the melt. (c) 3D direct simulations of temperature and flow patterns of thermal convection ($Gr = 2.86 \times 10^6$, $\Omega_s = \Omega_c = 0$).

bottom. However, a side heating mechanism of convection is dominated for $H > 4$ cm (area b in Fig. 3). This type of convection has a global feature and produces a transport from the crucible wall to the crystal. A very interesting and new result is interaction between these two types of convection which leads to significant destabilization in the region between a and b in Fig. 3 ($H \sim 3$ cm). We do not have enough space for discussing other interesting and complex effects of convection for a crucible with different geometry, for instance, for small height of the melt $H < 0.5$ cm, where two-dimensional (2D) and 3D cases are very different (Fig. 3, region a).

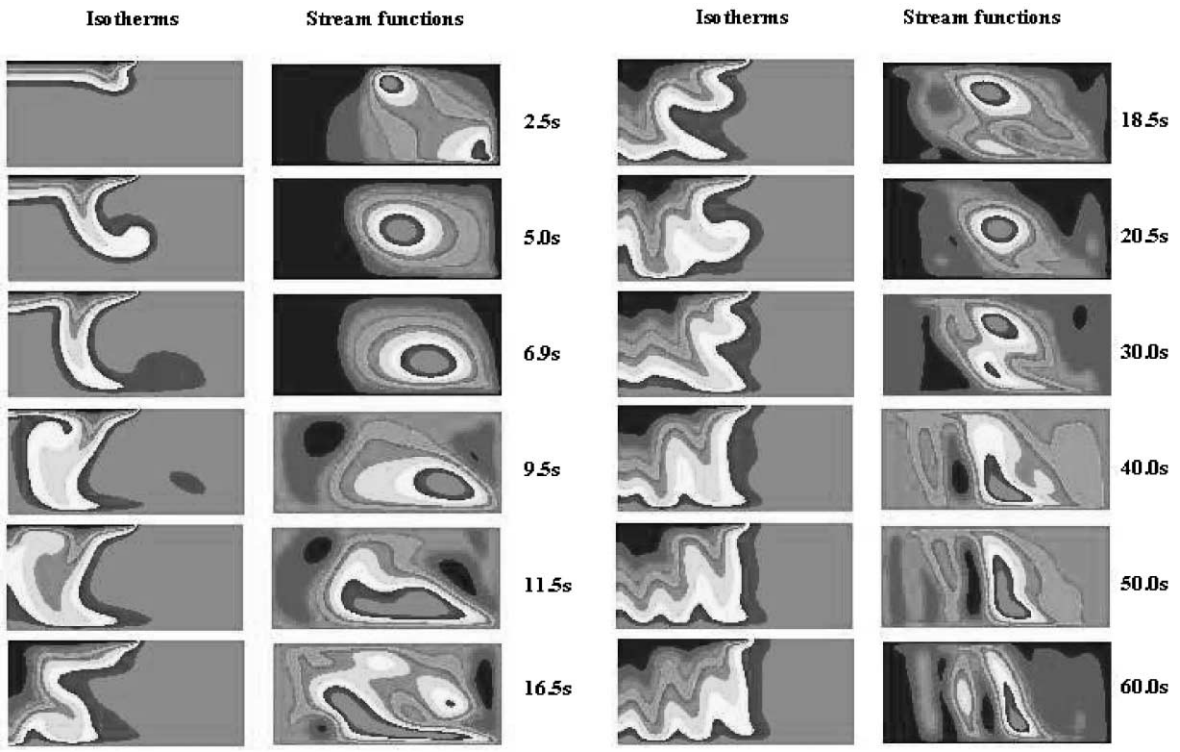

Fig. 4. Interaction of gravity-driven and forced convection: evolution of the thermal convection with crystal and crucible rotation in axisymmetric case ($\mathrm{Gr} = 7.8 \times 10^7$, $\Omega_s = 6$ rpm, $\Omega_c = -16$ rpm).

Fig. 4 shows one of the results of direct 3D simulations for basic height $H = 4$ cm (isotherms in azimuthal plane for small supercritical value of $\mathrm{Gr} = 2.85 \times 10^8$ for level $z = 0.75$). Finite difference control volume scheme and uniform mesh with $70 \times 64 \times 64$ grids was used for this case. The results of direct 3D simulations and stability analysis are very similar. Note that this structure named a "spoke type" structure, was observed in silicone melt in Ref. [26]. 3D calculation for low gravity $g/g_o = 0.01$, which corresponds to $\mathrm{Gr} = 7.8 \times 10^5$, shows steady state convection. It also confirms the conclusions of the linear stability analysis.

7. Coupling of the thermal convection and crystal/crucible rotation

Temporal evolution of the thermal convection with crystal and crucible rotation in axisymmetric case was demonstrated for 2D case using "INTEX" computer system. Following [9], an example with basic parameters: height $H = 4$ cm, $\mathrm{Gr} = 7.8 \times 10^7$, $\Omega_s = 6$ rpm, $\Omega_c = -16$ rpm, is typical for the growth of GaAs monocrystals. In this case, non-uniform mesh with 81×81 grids was used. One can see from Fig. 4 that thermals structure may be recognized in the early stage of the process, similar to the early stage (till about 7 s) for the case of thermal convection (Fig. 2). However, transient and long-term processes of coupling are quite different.

Oscillatory mechanism which may be recognized as W-type isotherms structure is realized for long-term duration in this figure. A qualitatively, similar instability has been discussed in the literature ([27] and references cited therein). However, the role of configuration and concrete parameters is very important. A significant feature of the flow field, in this case, in comparison with

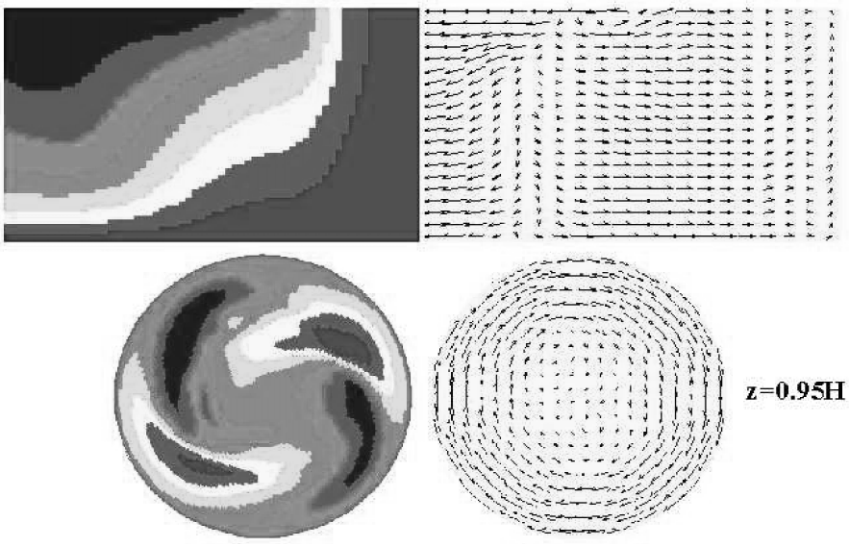

Fig. 5. Three-dimensional thermal convection with crystal and crucible rotation under reduced gravity ($Gr = 7.8 \times 10^5$, $\Omega_s = 6$ rpm, $\Omega_c = -16$ rpm).

long-term convection structure in Fig. 2 is the strong disturbances due to interaction with the forced type of convection. A parametrical analysis has been performed with the goal of investigating a mechanism related to the W-type of instability. A special run with thermal convection and only crystal rotation ($Gr = 7.8 \times 10^7$, $\Omega_s = 6$ rpm, $\Omega_c = 0$) shows small temperature oscillations. However, for the case of thermal convection and only crucible rotation ($Gr = 7.8 \times 10^7$, $\Omega_s = 0$, $\Omega_c = -16$ rpm), it is definitely shown that the main reason for the instability is a coupling between thermal convection and crucible rotation due to the high speed of crucible rotation. Note that the coupling effect strongly depends on the melt height and thermal regime of the bottom. For instance, paper [14] reports stabilization of a coupling flow for silicon growth configuration which is not confirmed for our configuration in 3D case. The rotation of the crucible for damping this type of the oscillations using 2D model was determined here to be about 1.5 rpm, which is close to the above mentioned critical value 1.2 rpm for 3D instability of crucible rotation. Note that the calculation which was done for basic case shows a developed chaotic regime.

Special calculations were carried out with the goal of investigating convection regime in low gravity with Gr number reduced to 7.8×10^5 in the case with rotation crystal and crucible $\Omega_s = 6$ rpm, $\Omega_c = -16$ rpm. Note that 2D coupling flow is close to a steady state regime. The result of calculations of 3D coupling flow is shown in Fig. 5. Spectral-finite difference scheme was used in this case with $64 \times 64 \times 64$ grids on uniform meshes. 3D flow is unsteady in this case. However, one can see from Fig. 5, that W-type isotherms structure in $r - z$ plane similar to that in Fig. 4, is absent. Moreover, temperature structure in r–z plane is qualitatively similar to the same case, but without thermal convection. Therefore, a low gravity with $g/g_o = 10^{-2}$–10^{-3} (with Gr number reduced to 7.8×10^5), probably may be enough for damping the most strongest instability. This result may be used as one of the possible explanations for the elimination of striation in microgravity.

8. Conclusions

As a result of modeling fluid flow in a crucible of idealized Czochralski method, critical speed

rotation of the crystal in 3D case for a given configuration is found to be $(\Omega_s)_c = 7.7$ rpm ($Re_s = 7.7 \times 10^3$) and crucible rotation $(\Omega_c)_c$ to be 1.2 rpm ($Re_c = 1.2 \times 10^3$).

Three different possible mechanisms of gravity-driven convection in crucible are shown: side heating, cooling from above near the crystal front, and bottom heating. Critical Grashof number for the onset of the temperature oscillations due to convective instability in a given configuration for basic height is found to be 1.5×10^8 for axisymmetric and 2.5×10^6 for 3D case. Dependency of these critical values on the height and boundary between different mechanisms of thermal gravity-driven convection are found. Coupling of convection and crucible rotation is the most strongest reason for instability which exists even in axisymmetric case.

The results of the paper give an estimate of the quantitative comparison between the effect of low gravity and low crucible rotation or symmetrization of the temperature/flow fields as important low energetic control actions which may be alternatives to expensive microgravity action for damping of the temperature oscillations in the melt with a goal to eliminate striations in semiisolating GaAs crystals.

Acknowledgements

This work was supported partly by the Ministry of Science and Technology of the Russian Federation under Project No. 0201.06.253 and RSA-NASA Project TM-11. Authors would like to acknowledge V.G. Kosushkin for the technological consulting and M.N. Miakshina for the help in calculations and graphics.

References

[1] W.E. Langlois, Buoyancy-driven flows in crystal-growth melts, Ann. Rev. Fluid Mech. 17 (1985) 191.
[2] F. Dupret, N. Van den Bogaert, Modelling Bridgman and Czochralski growth, in: D.T.J. Hurle (Ed.), Handbook of Crystal Growth, Vol. 2, Elsevier, Amsterdam, 1994, p. 875.
[3] Q. Xiao, J.J. Derby, J. Crystal Growth 152 (1995) 169.
[4] N.V. Nikitin, V.I. Polezhaev, Fluid Dyn. 34 (3) (1999) 322.
[5] N.V. Nikitin, V.I. Polezhaev, Fluid Dyn. 34 (6) (1999) 843.
[6] M.K. Ermakov, S.A. Nikitin, V.I. Polezhaev, Fluid Dyn. 32 (3) (1997) 338.
[7] V.I. Polezhaev, M.K. Ermakov, N.V. Nikitin, S.A. Nikitin, International Symposium on Advances in Computational Heat Transfer, 26–30 May, Cesme, Turkey, 1997, in: Advances in Computational Heat Transfer, Begell House, New York, 1998, p. 492.
[8] B.G. Zakharov, V.G. Kosushkin, N.V. Nikitin, V.I. Polezhaev, Fluid Dyn. 33 (1) (1998) 110.
[9] V.G. Kosushkin, V.I. Polezhaev, J. Mater. Sci. Mater. Electron. 10 (1999) 601.
[10] K. Kakimoto, M. Egughi, H. Watanabe, T. Hibiya, J. Crystal Growth 94 (1989) 415.
[11] A. Bottaro, A. Zebib, Phys. Fluids 31 (1988) 495.
[12] M.E. Sacudean, P. Sabhapathy, F. Weinberg, J. Crystal Growth 94 (1989) 522.
[13] J.-P. Fontaine, A. Randriamampianina, G.P. Extremet, P. Bontoux, J. Crystal Growth 97 (1989) 116.
[14] K. Kakimoto, M. Watanabe, M. Egughi, T. Hibiya, J. Crystal Growth 126 (1993) 435.
[15] A.D.W. Jones, J. Crystal Growth 69 (1984) 165.
[16] V.S. Berdnikov, V.L. Borisov, V.A. Markov, V.I. Panchenko, Laboratory modeling of the macroscopic transport processes in the melt during crystal growth by the pulling method, in: V.S. Avduevsky, V.I. Polezhaev (Eds.), Hydrodynamics, Heat and Mass Transfer during Material Processing, Vol. 68, Nauka, Moscow, 1990 (in Russian).
[17] D.K. Mukherjee, V. Prasad, P. Dutta, T.J. Yuan, J. Crystal Growth 169 (1996) 136.
[18] U. Krzyminski, A.G. Ostrogorsky, J. Crystal Growth 174 (1997) 19.
[19] A.A. Wheeler, J. Crystal Growth 102 (1991) 691.
[20] U. Buckle, M.J. Schaefer, J. Crystal Growth 126 (1993) 682.
[21] P. Santhana Raghavan, P. Ramasamy, in: H.J. Scheel (Ed.), First International School on Crystal Growth Technology, Beatenberg, Switzerland, 5–16 September, 1998, Book of Lecture Notes, p. 787.
[22] G.M. Guadalupi, F. Danieli, G. Tolomio, B. Molinas, M. Favaretto, L. Meregalli, in: H.J. Scheel (Ed.), First International School on Crystal Growth Technology, Beatenberg, Switzerland, 5–16 September, 1998, Book of Lecture Notes, p. 789.
[23] E.M. Sparrow, R.B. Husar, R.J. Goldstein, J. Fluid Mech. 41 (1970) 793.
[24] A.V. Bune, A.T. Ginzburg, V.I. Polezhaev, K.N. Fedorov, Izv. Atmos. Oceanic Phys. 21 (9) (1985) 736.
[25] V.I. Polezhaev, M.K. Ermakov, S.A. Nikitin, M.N. Miakshina, Mater. Electron. 1 (2000) 48 (in Russian).
[26] K.-W. Yi, K. Kakimoto, M. Egughi, M. Watanabe, T. Shyo, T. Hibiya, J. Crystal Growth 144 (1994) 20.
[27] J.R. Ristorcelli, J.L. Lumely, J. Crystal Growth 116 (1992) 447.